JOURNAL OF SOLID STATE CHEMISTRY 117, 21–29 (1995)

Ordering and Defects in $BaMnO_{3-y}$ ($0.22 \leq y \leq 0.40$)

M. Parras,* J. Alonso,† J. M. González-Calbet,*,† and M. Vallet-Regí†,‡

*Departamento Química Inorgánica, Facultad de Químicas, Universidad Complutense, 28040 Madrid, Spain; †Instituto de Magnetismo Aplicado (RENFE-UCM), Apdo. 155, 28230 Las Rozas, Madrid, Spain; and ‡Departamento de Química Inorgánica y Bioinorgánica, Facultad de Farmacia, Universidad Complutense, 28040 Madrid, Spain

Received August 4, 1994; in revised form October 27, 1994; accepted October 30, 1994

An electron diffraction and high resolution electron microscopy study shows that nonstoichiometry in $BaMnO_{3-y}$ ($0.22 \leq y \leq 0.40$) perovskite-related materials is accommodated either by means of disordered intergrowths of hexagonal $BaMnO_{3-y}$ polytypes for $0.22 \leq y < 0.25$ or by random distribution of anionic vacancies for $0.25 < y \leq 0.40$. For $y = 0.25$, an ordered 4H-$Ba_4Mn_4O_{11}$ phase is obtained with stacking sequence ... hchc .... Structural models for the 4H type showing ordering of vacancies along the cubic layer are discussed. © 1995 Academic Press, Inc.

INTRODUCTION

In a series of previous papers (1–5) we have stated that oxygen deficiency in $BaMnO_{3-y}$ ($0 < y < 0.25$) is accommodated by the introduction of $BaO_{2.5}$ cubic layers in the hexagonal close-packing characteristic of Ba MnO_{3-y}, ordered phases being obtained for $y = 0.5c/(c + h)$ where c and h refer to the number of cubic and hexagonal layes per unit cell, respectively.

The 2H-$BaMnO_3$ perovskite-related oxide is formed by a hexagonal stacking sequence of BaO_3 layers (6). A powder X ray diffraction study by Negas and Roth (7) shows that oxygen deficiency in $BaMnO_{3-y}$ leads to the formation of 15R-, 8H-, 6H-, 10H-, and 4H-$BaMnO_{3-y}$ as a consequence of the different stacking sequence of hexagonal and cubic layers.

$BaMnO_{3-y}$ materials prepared by accurate control of the oxygen content and characterized by electron diffraction (ED) and high resolution electron microscopy (HREM) prove the existence of two domains in the Ba MnO_{3-y} ($0 < y < 0.25$) system. For $0 < y \leq 0.1$, compositional variations are accommodated either by means of formation of ordered rhombohedral phases, as 21R (4) and 15R (5), or by means of disordered intergrowths of these and other rhombohedral types (27R, 33R) as shown by HREM (3–5).

On the other hand, only hexagonal types (8H, 10H, 6H, and 4H) intergrow in the compositional range $0.1 < y \leq 0.25$ which can be isolated as a function of both the oxygen content and the synthesis procedure (1, 2). Table 1 summarizes the different structural types up to now described in the $BaMnO_{3-y}$ system.

Samples with $y < 0.25$ have not been reported thus far. We describe in this paper the accommodation of nonstoichiometry in the compositional range $0.22 < y < 0.40$.

EXPERIMENTAL

Oxygen deficiency in the reduction process of 2H-$BaMnO_3$ hexagonal type leads to the introduction of $BaO_{2.5}$ cubic layers and then to the modification of the initial hexagonal close packing. By an accurate control of both pressure and temperature along the reduction process of $BaMnO_{3-y}$, samples with a given value of y can be isolated. Mass loss data obtained from temperature-reduced program studies at a constant heating rate are used to determine the oxygen content of the starting material as well as the existence of intermediate compounds from a plateau or inflection point of the so-obtained thermogram.

$BaMnO_{3-y}$ materials were obtained by using a thermogravimetric analysis system built on the basis of a Cahn D-200 electrobalance which operates under static atmosphere. An electric furnace enables operating from room temperature to 1000°C and, due to the excellent sensibility of the electrobalance, the oxygen content can be determined, for instance, within $\pm 2 \times 10^{-3}$ for a $BaMnO_{3-y}$ sample of a total mass of about 100 mg. The vacuum and the gas blending system allow one to operate with a gas mixture at a given total pressure.

From $BaMnO_3$ (2H) as starting material, the following samples have been prepared:

(i) $BaMnO_{2.78}$ was obtained by heating $BaMnO_3$ at 900°C in a vacuum. When a value of $y = 0.22$ was reached in the thermobalance, the sample was annealed at 400°C for 12 hr. Under these conditions, the weight sample remains constant.

[1] To whom correspondence should be addressed.

0022-4596/95 $6.00

TABLE 1
Structural Types up to Now Described in the $BaMnO_{3-y}$ System

Type	Chemical composition	Stacking sequence	Reference
2H	$BaMnO_3$	... hhh ...	6, 7
33R	[a]	... $(chhhhhhhhhh)_3$ ...	3
27R	[a]	... $(chhhhhhhh)_3$ ...	3
21R	$BaMnO_{2.928}$	... $(chhhhhh)_3$ ...	4, 5
15R	$BaMnO_{2.90}$	... $(chhhh)_3$ ...	4, 7
8H	$BaMnO_{2.875}$	... $(chhh)_2$ ...	7
8H'	[a]	... chhhhhch ...	1, 2
6H	$BaMnO_{2.83}$	... chhhch ...	1, 2, 7
10H	$BaMnO_{2.80}$	... $(chchh)_2$ ...	7
4H	$BaMnO_{2.75}$	... chch ...	7

[a] Only observed as isolated lamellae by HREM. The theoretical composition should be 33R-$BaMnO_{2.954}$, 27R-$BaMnO_{2.944}$, and 8H'-$BaMnO_{2.875}$.

(ii) $BaMnO_{2.75}$ was obtained by reducing $BaMnO_3$ in argon in the electrobalance. The $y = 0.25$ composition was reached at 1300°C. Then the sample was cooled to room temperature.

(iii) $BaMnO_{2.60}$ was synthesized in the thermobalance by reducing $BaMnO_3$ under a mixture of He/H_2 (0.45 atm/0.05 atm) and heating at a constant rate of 1°C/min up to 500°C, i.e., when the $y = 0.40$ composition was reached. Then the sample was annealed at 500°C for 3 hr keeping the weight constant.

Powder X ray diffraction was performed on a SIEMENS D-5000 diffractometer equipped with a secondary graphite monocromator and using Cu$K\alpha$ radiation.

Electron diffraction was carried out on a JEOL 2000FX electron microscope, fitted with a double-tilting goniometer stage (±45°). High resolution electron microscopy was performed on a JEOL 4000 EX electron microscope fitted with a double-tilting stage (±25°), by working at 400 Kv.

RESULTS AND DISCUSSION

The 4H-$Ba_4Mn_4O_{11}$ Phase

The powder X ray diffraction pattern corresponding to the $BaMnO_{2.75}$ sample is shown in Fig. 1. All diffraction maxima can be indexed on the basis of a unit cell of hexagonal symmetry characteristic of the 4H-structural type and parameters $a = 0.567$ nm, $c = 0.932$ nm, in good agreement with the results previously reported by Negas and Roth (7).

Figures 2a and 2b show the electron diffraction pattern along [010] zone axis and the corresponding high resolution electron micrograph. An ordered material is obtained for the $BaMnO_{2.75}$ composition which is in agreement with the structural model corresponding to the 4H type (Fig. 2c). Since the stacking sequence for such a structural model is ... hchc ..., this is a new example proving that oxygen deficiency in $BaMnO_{3-y}$ is accommodated by the introduction of $BaO_{2.5}$ cubic layers in the hexagonal close packing of the $BaMnO_3$ according to the expression $y = 0.5c/(c + h)$ (3).

Several $A_4Mn_4O_{11}$ perovskite-related phases have been described. For A = Ca (8) or La (9) a cubic close packing is obtained. The reduction process from $AMnO_3$ leads to different coordination for Mn as a function of the A cation oxidation state. Thus, for A = Ca, Mn^{3+} is stabilized in square pyramidal sites (8). For A = Ln, Mn^{2+} occupies tetrahedral sites (9).

On the other hand, Negas and Roth (10) have previously studied some aspects related to the nonstoichiometry in the 4H structural type corresponding to the $SrMnO_{3-y}$ system. The ideal 4H-type structure presents a stacking sequence ... ABCB ... (... hchc ...) of AO_3 layers along the c axis. According to Negas and Roth (10) the introduction of one AO_2 layer every four layers per unit cell is necessary to reach a $SrMnO_{2.75}$ composition. If an A-layer oxygen is removed, the result is two nonbinding, Mn^{3+} trigonal bipyramids, each sharing a face with a Mn^{4+} octahedron. If a B- or C-layer oxygen position is vacant, then two distorted Mn^{3+} trigonal bipyramids sharing an edge are created. In both cases, this leads to a sequence of AO_2–AO_3–AO_3–AO_3 layers per unit cell, where AO_2 can be either a cubic or a hexagonal layer.

Such a model is not consistent with the introduction of $AO_{2.5}$ cubic layers as responsible for the accommodation of nonstoichiometry. To remove oxygens leading to an $AO_{2.5}$ composition many possibilities arise. By looking at an AO_3 hexagonal layer (Fig. 3a), one possibility is, for instance, to remove one oxygen in a similar way to that proposed by Shibahara (Fig. 3b) for $BaNiO_x$ (11). These anionic vacancies originate 50% of pyramidal environ-

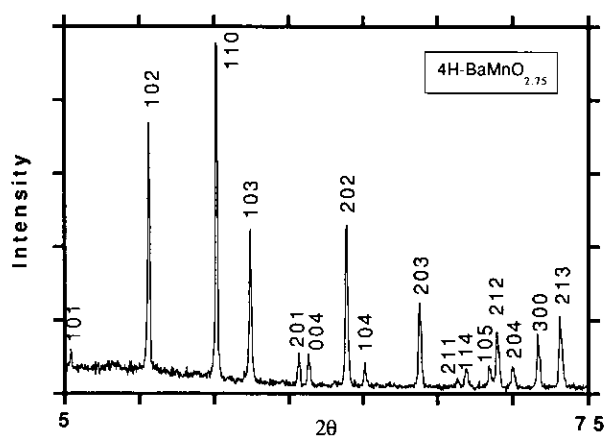

FIG. 1. Powder X ray diffraction pattern corresponding to $BaMnO_{2.75}$.

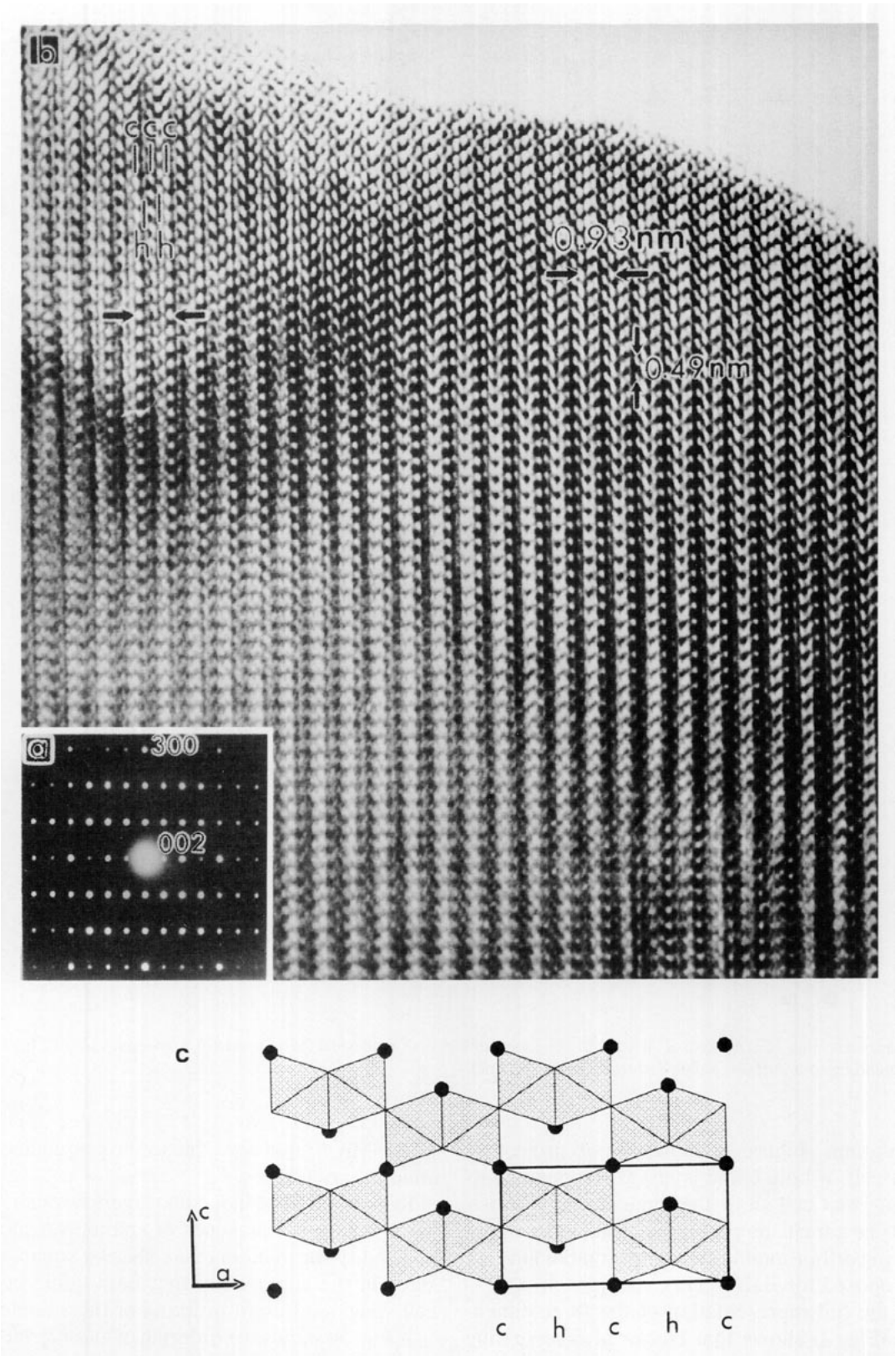

FIG. 2. (a) Electron diffraction pattern of $BaMnO_{2.75}$ along [010]. (b) Corresponding high resolution electron micrograph. (c) Structural model corresponding to the 4H structural type.

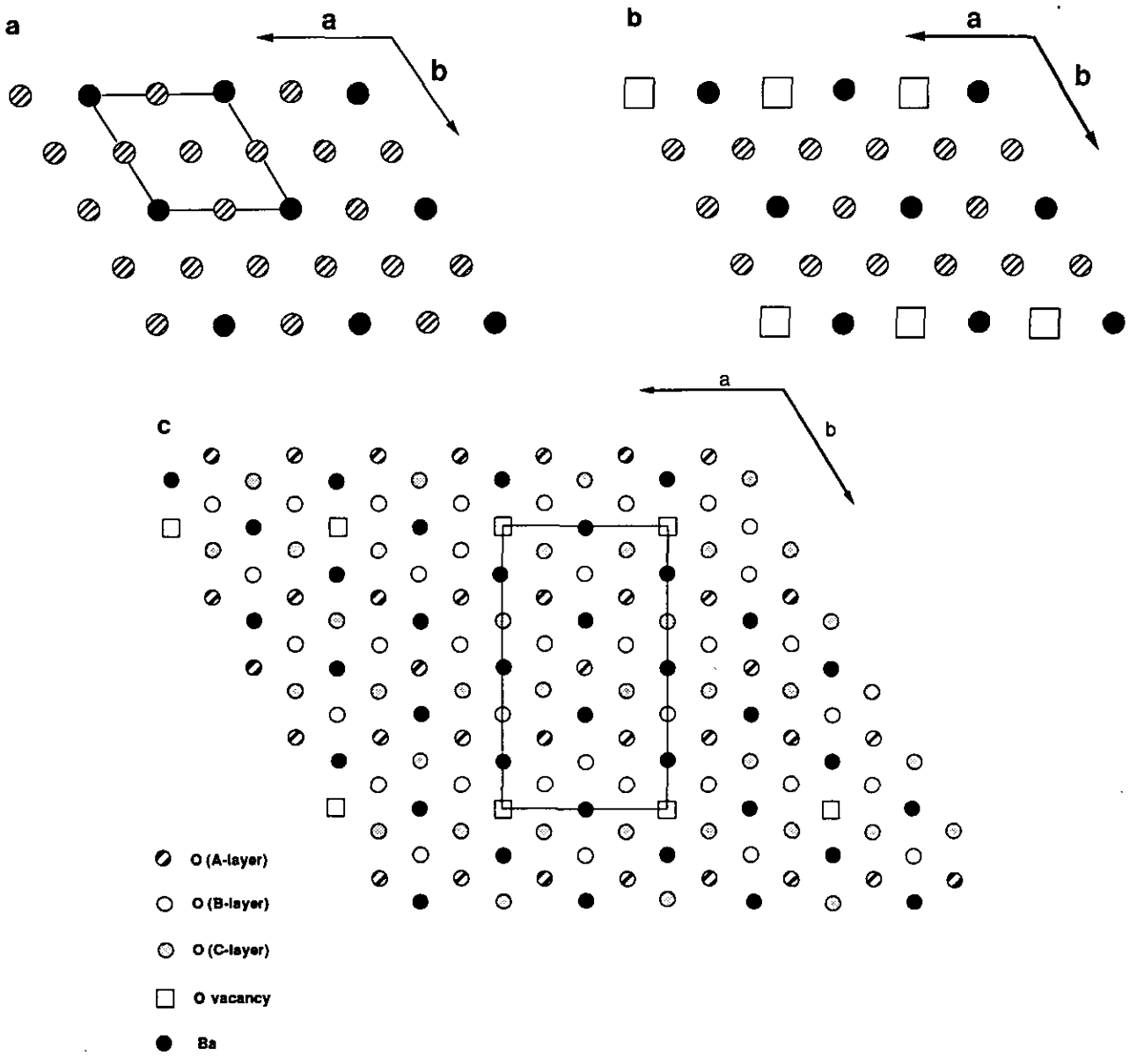

FIG. 3. (a) Representation of a hexagonal AO_3 layer. (b) Representation of a possible $AO_{2.5}$ layer (□ = oxygen vacant). (c) Projection along the c-axis corresponding to an orthorhombic distortion of 4H-$BaMnO_{2.75}$.

ments for Mn atoms. Figure 3c shows the *ab* projection of such a unit cell. If both cubic layers corresponding to the ... chch ... unit cell show the same atomic disposition, the 4H type cannot be preserved, leading to a new unit cell showing orthorhombic symmetry (marked in Fig. 3c) as that proposed for $BaIrO_3$ (12).

Moreover, the full representation of the three-dimensional model (Fig. 4) shows that blocks of face-sharing square pyramids and face-sharing octahedra are linked by sharing vertices along the c axis. However, this is not a plaussible model since $AO_{2.5}$ cubic layers are introduced in the hexagonal close packing to minimize the Mn^{3+}–Mn^{3+} repulsions due to the presence of square pyramids sharing faces.

Keeping in mind that cubic layers have an $AO_{2.5}$ composition due to the presence of anionic vacancies, the only possibility for avoiding face-sharing square pyramids resides in the supposition that both cubic layers per unit cell show a different ordering of the anionic vacancies.

If Fig. 5a shows the ordering of anionic vacancies corresponding to one of the cubic layers, for instance, at z = 0, which in the following will be called the c_1 layer, the cubic layer at z = 1/2, c_2, should be that represented in Fig. 5b, where oxygen vacancies are alternating with

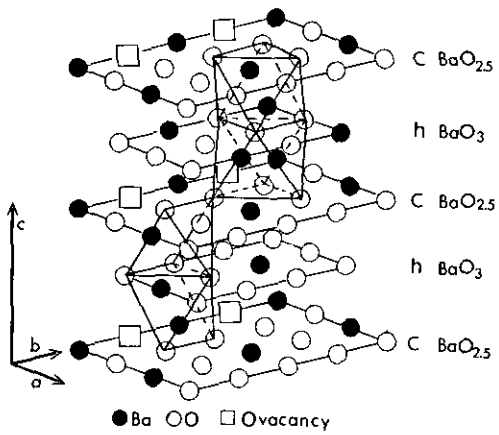

FIG. 4. Three-dimensional model corresponding to the previous orthorhombic cell.

respect to the previous cubic layer. This alternance leads to the structural model proposed in Fig. 5c in which blocks constituted by one pyramid and one octahedron sharing faces are linked to similar blocks sharing vertices along the c axis. However, such a structural model should lead to a doubling of the a axis corresponding to the 4H cell, as a consequence of a stacking sequence ... $c_1hc_2hc_1hc_2$ h .... In order to avoid such a doubling of the unit cell, it is necessary to suppose that the c_1 and c_2 cubic layers are not always orderly alternating along the c axis. A similar disordered disposition of anionic vacancies in $AO_{2.5}$ layers has been previously described in the Ba FeO_{3-y} system (13).

Random Distribution of Anionic Vacancies in $BaMnO_{2.60}$

Powder X ray diffraction data corresponding to this material are similar to those shown for $BaMnO_{2.75}$. However, a slight deviation of all maxima is observed leading to an increase of the unit cell (a = 0.570 nm, c = 0.938 nm) as a consequence of a decrease of Mn^{4+}. In order to study the accommodation of anionic vacancies, an electron microscopy study was performed. All crystals show electron diffraction patterns corresponding to the 4H-type structure. The majority of crystals are ordered showing images along [010] similar to that shown in Fig. 2b. However, a certain kind of defect, previously observed in 4H-$SrMnO_{3-y}$ (14), is detected in a minority of crystals as shown in the micrograph along the [010] zone axis (Fig. 6).

The planar defect could be characterized by the fact that the interface with stacking fault appearing in the bright contrast in the observed image of Fig. 6 is intersected at an angle of about 30° to the c axis of the 4H structure. The stacking sequence on the boundary where the displacement has taken place, with the vector of $\pm 1/3\ [1\bar{1}0]$ in the hexagonal unit cell, involves a corner-sharing MnO_6 octahedra. This displacement results from the introduction of an excess of cubic $AO_{2.5}$ layers with respect to the 4H type (Fig. 7).

In any case, such a small amount of defects does not justify the strong difference in oxygen stoichiometry from $BaMnO_{2.75}$ to $BaMnO_{2.60}$. A reduction of $BaMnO_{2.75}$ leads to the introduction of new cubic $AO_{2.5}$ layers in the ... chch ... sequence characteristic of the 4H structural type, which obviously implies the presence of adjacent cubic layers. Due to the small amount of defects showing this disposition of cubic layers, it must be supposed that this is not the most stable way of accommodation of anionic vacancies.

In fact, the diffraction data suggest that this material keeps the 4H structural type despite the strong anionic deficiency with respect to $BaMnO_{2.75}$, according to which, compositional variations in $BaMnO_{2.60}$ should be accommodated by random distribution of anionic vacancies. If oxygen atoms are removed from a $BaO_{2.5}$ cubic layer, a composition close to BaO_2 should result, leading to Mn atoms in tetrahedral coordination which is quite an extraordinary coordination for trivalent manganese. For this reason, the most probable situation results from the elimination of oxygen atoms from hexagonal BaO_3 layers. To obtain $BaMnO_{2.60}$ composition, the average composition of the hexagonal layers should be $BaO_{2.7}$, thus indicating that 80% of Mn atoms are in square pyramidal coordination. It is worth recalling that in the $SrMnO_{3-y}$ system, Negas and Roth (10) suggested that the basic 4H structure remains stable as the number of missing oxygens approachs one per 4H unit cell ($SrMnO_{2.75}$), at which point transformation to a perovskite (... ABC ... layer sequence) must occur. According to our results, the situation is quite different in the $BaMnO_{3-y}$ system. If such a transformation occurs, it should take place at a composition lower than $BaMnO_{2.60}$, thus indicating that the number of missing oxygens should be higher than 1.6 per 4H unit cell. New reduction experiments in the $BaMnO_{3-y}$ system for $0.4 < y \leq 0.5$ are in progress.

Disordered Intergrowth in $BaMnO_{2.78}$

The powder X ray diffraction pattern corresponding to this material is similar to that shown by $BaMnO_{2.75}$. No changes are appreciated in the unit cell parameters. However, the electron diffraction study suggests a more complicated situation.

Although many crystals show electron diffraction patterns corresponding to the 4H type, some others present a high concentration of defects. Figure 8a shows the electron diffraction pattern along [010]. The streaking observed along the c axis is clearly reflected in the corresponding high resolution electron micrograph (Fig. 8b).

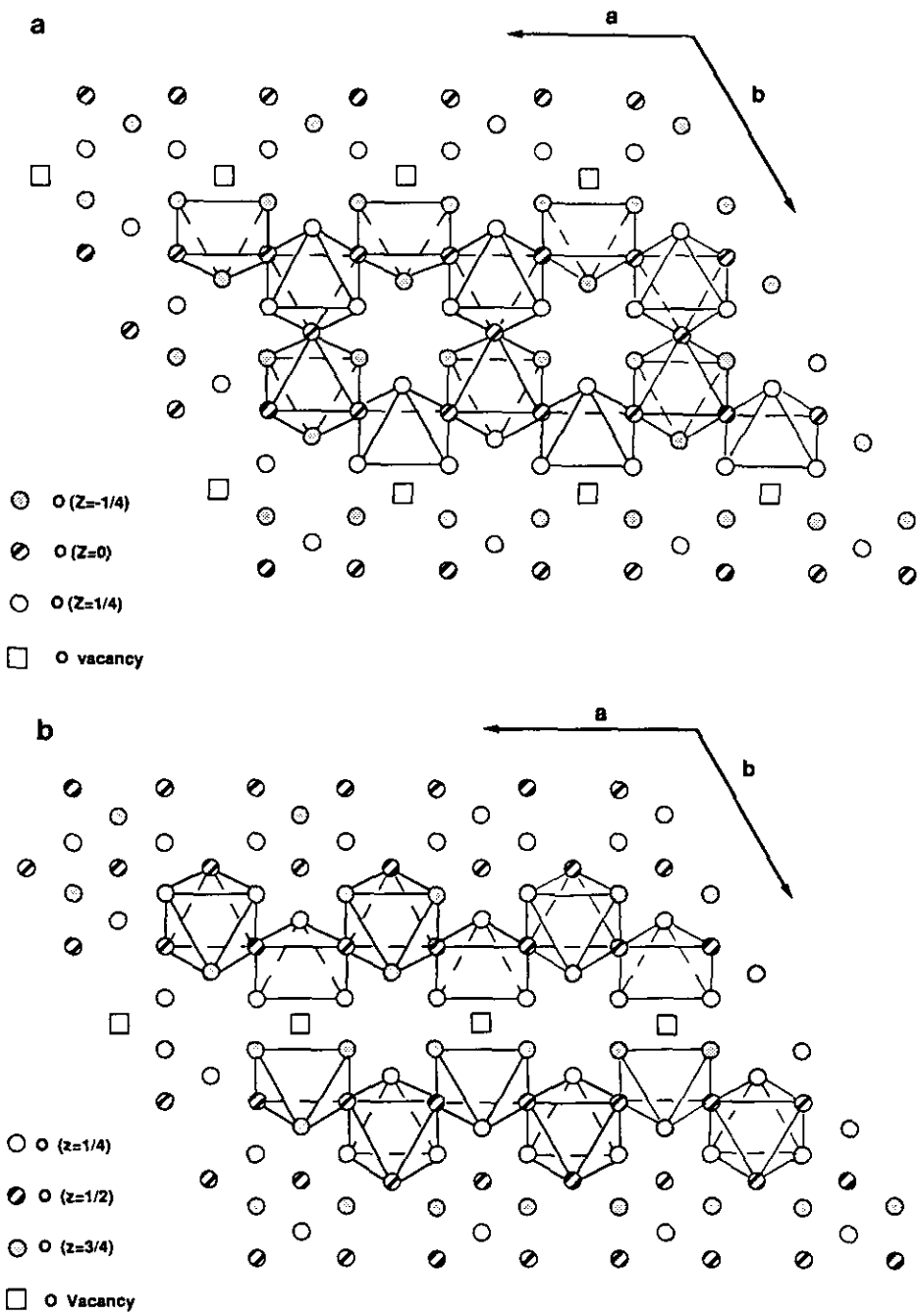

FIG. 5. (a) Ordering of anionic vacancies in the cubic layer at $z = 0$. (b) Ordering of anionic vacancies in the cubic layer at $z = 1/2$. (c) Structural model proposed for 4H-$BaMnO_{2.75}$.

As can be observed, cubic and hexagonal layers intergrow in a disordered way, only the ... chch ... and ... chhhch ... stacking sequences corresponding to 4H-$BaMnO_{2.75}$ and 6H-$BaMnO_{2.83}$ (2) being clearly appreciated.

This is a new example corresponding to the $BaMnO_{3-y}$ system showing that the accommodation of compositional variations only leads to ordered phases for a given y value, intermediate values giving rise to disordered intergrowth of the closest stable phases. Regarding the average composition of this material, $BaMnO_{2.78}$, such phases are $BaMnO_{2.75}$ and $BaMnO_{2.80}$ (10H-type) (7). However, despite that the composition is close to $BaMnO_{2.80}$ there is no evidence of a stacking sequence ... $(hhchc)_2$ ...

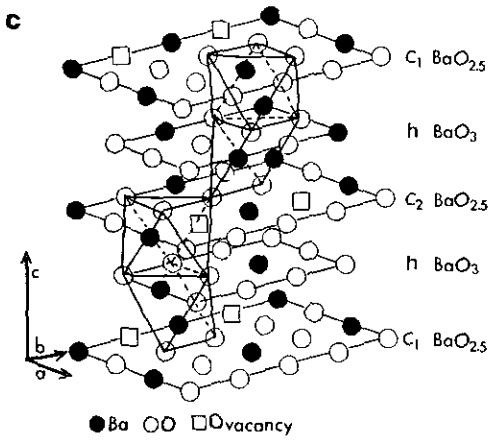

FIGURE 5—*Continued*

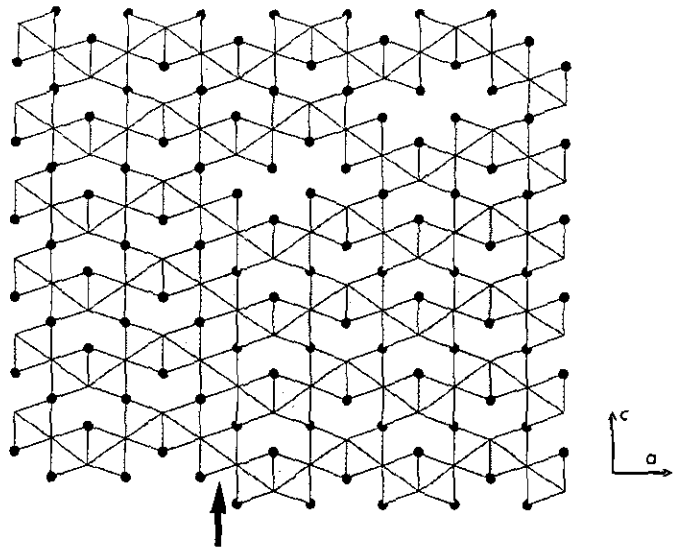

FIG. 7. Structure model of the planar defect involving the introduction of an extra cubic $AO_{2.5}$ layer.

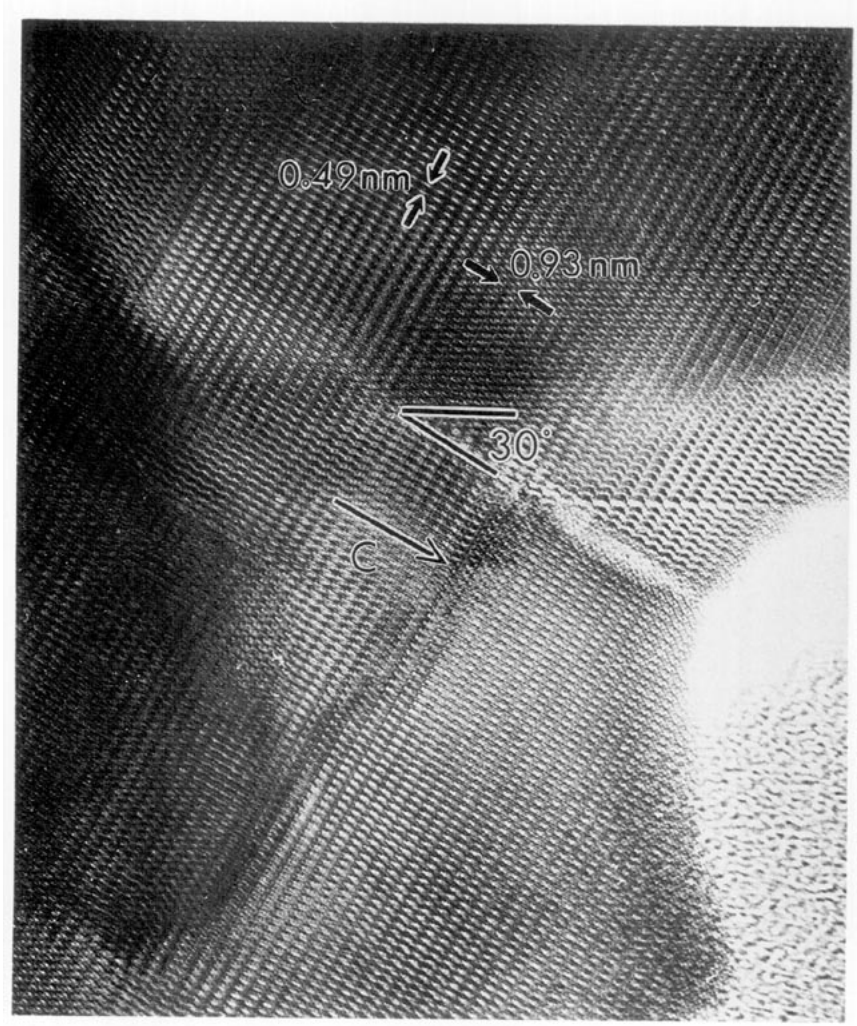

FIG. 6. Electron micrograph of $BaMnO_{2.60}$ along [010]. A planar defect is apparent.

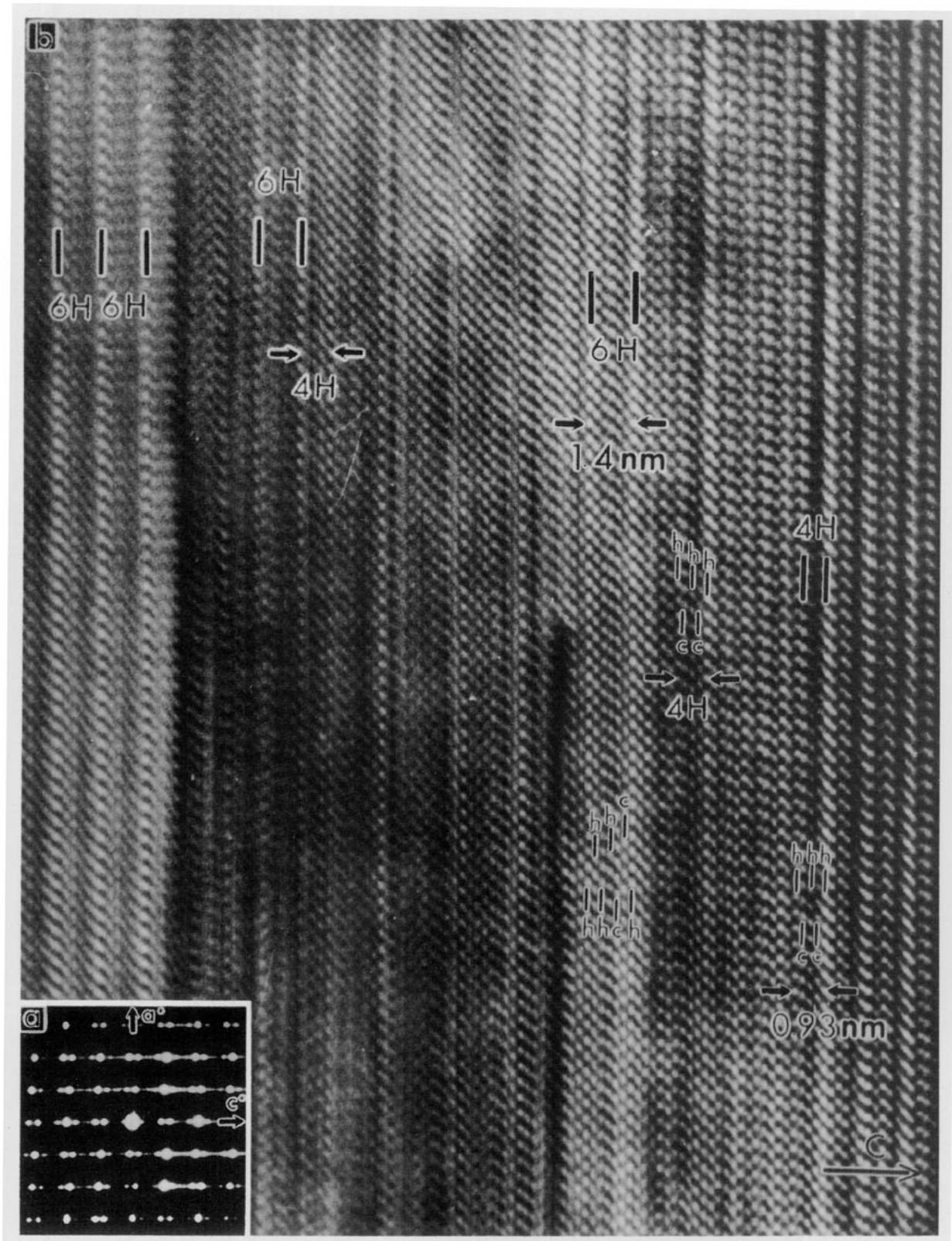

FIG. 8. (a) Electron diffraction pattern of $BaMnO_{2.78}$ along [010]. Streaking along the c axis is apparent. (b) Corresponding high resolution micrograph showing disordered intergrowth of both 4H and 6H structural types.

characteristic of the 10H-type. Moreover, previous attempts to isolate the $BaMnO_{2.80}$ compound have originated disordered materials, thus indicating that thermodynamic conditions for isolating such a material must be very narrow (15).

On the basis of this and previous reports, it can be concluded that compositional variations in the $BaMnO_{3-y}$ system are accommodated in different ways as a function of the oxygen concentration. Thus, for $0 < y \leq 0.1$, two rhombohedral phases have been isolated for $y = 0.07$ and 0.10, intermediate values giving rise to disordered intergrowths of rhombohedral phases. For higher concentration of anionic vacancies, $0.1 < y \leq 0.25$, several hexagonal phases have been described, 8H, 6H, 10H, and 4H, showing the composition $BaMnO_{2.875}$, $BaMnO_{2.83}$, $BaMnO_{2.80}$, and $BaMnO_{2.75}$. Once again, intermediate values of the oxygen content give rise to disordered intergrowths of these hexagonal types. However, for $0.25 < y \leq 0.40$, anionic vacancies are randomly distributed keeping the 4H type corresponding to $BaMnO_{2.75}$.

ACKNOWLEDGMENTS

Financial support of CICYT (Spain) through Research Projects MAT91-0331 and MAT93-0207 are acknowledged. We are also grateful to Mr. J. L. Baldonedo and Mr. E. Baldonedo for valuable technical assistance.

REFERENCES

1. M. Parras, J. Alonso, J. M. González-Calbet and M. Vallet-Regí, *Solid State Ionics* **63–65,** 614 (1993).
2. J. M. González-Calbet, M. Parras, J. Alonso, and M. Vallet-Regí, *J. Solid State Chem.* **106,** 99 (1993).
3. J. M. González-Calbet, M. Parras, J. Alonso, and M. Vallet-Regí, *J. Solid State Chem.* **111,** 202 (1994).
4. J. M. González-Calbet, M. Parras, J. Alonso, and M. Vallet-Regí, "Electron Microscopy 1994, Paris, Proceedings of the 13th International Congress on Electron Microscopy" (B. Jouffrey and C. Colliex, Eds.), Vol. 2, p. 913. Les Editions de Physique, 1994.
5. M. Parras, J. M. González-Calbet, J. Alonso, and M. Vallet-Regí, *J. Solid State Chem.* **113,** 78 (1994).
6. A. Hardy, *Acta Crystallogr.* **15,** 179 (1962).
7. T. Negas and S. Roth, *J. Solid State Chem.* **3,** 323 (1971).
8. A. Reller, J. M. Thomas, D. A. Jefferson, and M. K. Uppal, *Proc. R. Soc. London Ser. A* **394,** 223 (1984).
9. J. A. M. Van Roosmalen and E. H. P. Cordfunke, *J. Solid State Chem.* **93,** 212 (1991).
10. T. Negas and S. Roth, *J. Solid State Chem.* **1,** 409 (1970).
11. H. Shibahara, *J. Solid State Chem.* **69,** 81 (1987).
12. P. L. Gai, A. J. Jacobson, and C. N. R. Rao, *Inorganic Chem.* **15**(2), 480 (1976).
13. M. Parras, M. Vallet-Regí, J. González-Calbet, and J. C. Grenier, *J. Solid State Chem.* **83,** 121 (1989).
14. H. Shibahara, *J. Mater. Res.* **6**(3), 565 (1991).
15. K. Uematsu, K. Kuroda, N. Mizutani, and M. Kato, *J. Am. Ceram. Soc.***60**(9–10), 466 (1977).